Time-of-Flight Pixel with Homodyne Phase Demodulation in Standard CMOS Technology

J. Illade-Quinteiro, P. López, V.M. Brea, D. Cabello
Centro Singular de Investigación en Tecnoloxías da Información (CiTIUS)
University of Santiago de Compostela
Spain
Email: julio.illade, p.lopez, victor.brea, diego.cabello@usc.es

***Abstract*—This paper presents an indirect Time-of-Flight sensor for standard CMOS technologies with an alternative demodulation scheme based on homodyne techniques. This avoids control signals shorter than the period of the emitted light signal, which prevents synchronization issues and minimizes switching effects like charge injection and clock feedthrough. The feasibility of the pixel and the demodulation scheme is demonstrated through simulations.**

I. Introduction

Time-of-Flight (ToF) cameras are distance sensors that calculate the entire 3-D information of a scene. Their operation method is to illuminate the scene with, usually infrared, light signals and measure the time it takes to travel back and forth from the target. Indirect ToF sensors working with continuous wave (CW) apply sinusoidal modulation to the light signal [1]. In such systems the distance information, d, is contained in the phase change between the emitted and the received signals, ϕ, and it can be calculated as:

$$d = \frac{c}{2}\frac{T\phi}{2\pi} \tag{1}$$

where c is the speed of light and T the period of the emitted signal. The maximum distance that the system can unambiguously calculate is proportional to T. On the other hand, longer T values lead to worse results in terms of signal-to-noise ratios [2], [3]. The values generally used for T in ToF are around 50 ns or less.

The most common scheme to calculate ϕ in modulated ToF sensors [4] involves integrating this light signal in four different time intervals for every signal period. The small values of the integration windows come with some problems associated, specially if standard CMOS technologies are used. First, careful generation and synchronization of the control signals for the four integration windows are necessary. In addition, the degradation of the obtained information due to switching effects [5] should be accounted for. In topologies like the ones in [6], where a pinned photodiode with several transmission gates are used for the demodulation, these effects do not appear due to the difference of potential between the photodiode and the floating capacitances. However, these topologies need the use of non-standard technologies.

The proposed pixel in this paper is based on homodyne techniques. This avoids short integration windows. To the best knowledge of the authors this type of demodulation for ToF sensing was only presented in [7]. Circuit realizations of such an idea have not been done since then. The main idea is to multiply the received sinusoidal signal by the originally emitted one. The result includes a DC addend proportional to the phase difference between the emitted and the received signal and a set of sinusoids with frequencies equal to the original one or harmonics of it. By filtering out the sinusoids, the phase difference ϕ can be retrieved.

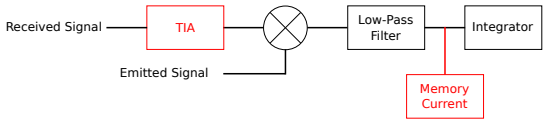

Fig. 1. System level diagram of the proposed demodulation principle.

II. Demodulation Principle of Operation

A system level block diagram of the proposed demodulation principle is shown in Fig. 1. The blocks in black show the basic parts common to all the systems that perform this demodulation and the blocks in red are contributions of our specific pixel implementation. Here it is assumed that the emitted and received signals are sinusoidal ones with the same period, T, and a phase difference of ϕ:

$$X_{received} = X_0 sin\left(\omega t - \phi\right) \tag{2}$$

$$X_{emitted1} = X_1 sin\left(\omega t\right) \tag{3}$$

where X_0 and X_1 are the received and emitted amplitudes.

The first step in the demodulation procedure is to use a mixer to multiply the emitted and received signals. The output of the mixer will then be:

$$X_{mixer} = \frac{-X_0 X_1}{2}\left[cos\left(\phi\right) + cos\left(2\omega t - \phi\right)\right] \tag{4}$$

As it can be seen this output have two components, a continuous one that carries the phase information and one at twice the frequency of the emitted signal. The output of the low-pass filter will be:

$$X_{LP} = -H_0\frac{X_0 X_1}{2}cos\left(\phi\right) \tag{5}$$

where H_0 is the DC gain of the low-pass filter. Integrating this signal for a time interval of T_{int} will give a signal at the output of the integrator of:

$$X_{INT} = \int_0^{Tint} X_{LP} dt = -\frac{H_0 X_0 X_1 T_{int}}{2} cos\left(\phi\right) \quad (6)$$

If instead using the emitted signal (3) as input to the mixer we use one with a phase difference of 90° with it:

$$X_{emitted2} = X_1 sin\left(\omega t + 90°\right) = X_1 cos\left(\omega t\right) \quad (7)$$

equation (6) is modified to:

$$X_{INT2} = -\frac{H_0 X_0 X_1 T_{int}}{2} sin\left(\phi\right) \quad (8)$$

and ϕ can be calculated as:

$$\phi = atan\left(\frac{X_{INT2}}{X_{INT}}\right) \quad (9)$$

Our pixel has a few differences with respect to the operation explained above. The blocks in red in Fig. 1 are the extra parts necessary in our circuit. These blocks are, first, a transimpedance amplifier (TIA) so the received signal can be converted into a voltage one, and, secondly, a current memory between the low-pass filter and the integrator to remove DC components that do not provide information about ϕ.

III. Pixel Topology

A ToF pixel in 180 nm standard CMOS technology was designed to prove the feasibility of the demodulation technique. Fig. 2 shows the schematic of the pixel. The five blocks described in the previous section are highlighted in different colors. The equations presented in the last section only considered the small signal components. Neverheless, the DC values of each signal have also to be considered. For example, the emitted signals used as input to the mixer were described with (3) and (7) but with the DC components of the signal these equations have to be rewritten as:

$$v_{CLK1} = V_{CLK} + v_{clk} sin\left(\omega t\right) \quad (10)$$

$$v_{CLK2} = V_{CLK} + v_{clk} cos\left(\omega t\right) \quad (11)$$

A. Transimpedance Amplifier

The background and received light signal are converted into a current by the sensing photodiode. This current is converted into a voltage signal by the TIA, highlighted in pink in Fig. 2. As it can be seen, its feedback resistance, R, is implemented by transistor MR in the triode region. The equivalent of (2) in our circuit will be:

$$v_{SIGN} = V_{SIGN} + v_{s0} sin\left(\omega t - \phi\right) \quad (12)$$

where V_{SIGN} is the DC component and includes the response of the circuit to the background light and v_{s0} the amplitude of the small signal component.

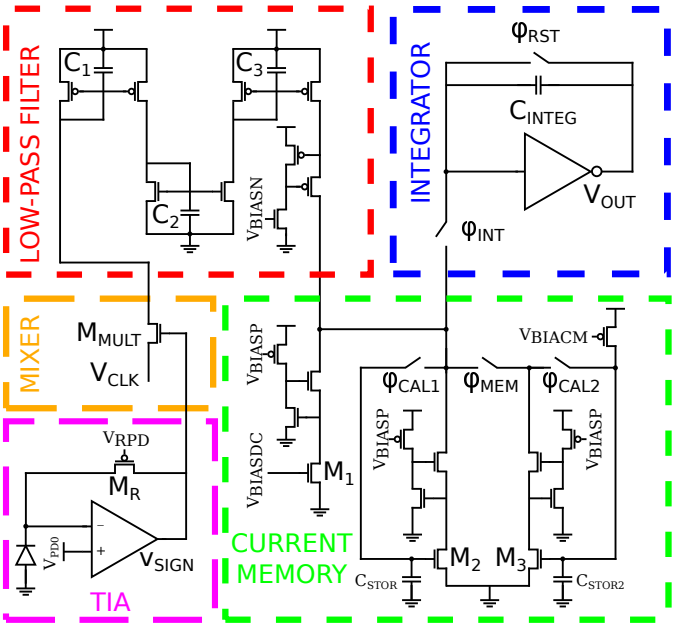

Fig. 2. Designed ToF pixel.

B. Mixer

The mixer circuit is implemented with a MOS transistor in the subthreshold region with the received and emitted signals applied to the gate and source terminals respectively. Assuming that V_{DS} is large enough, typically larger than 0.1 V, the current being drawn by this transistor will be:

$$i_{MULT} = I_0 exp\left(\frac{v_{SIGN} - v_{CLK1} - V_{THN}}{\eta V_T}\right) \quad (13)$$

where I_0 is the saturation current, V_{THN} the threshold current, η a process parameter and V_T the thermal voltage. We can define:

$$\tilde{I}_0 = I_0 exp\left(\frac{V_{SIGN} - V_{CLK} - V_{THP}}{\eta V_T}\right) \quad (14)$$

and, assuming the sinusoidal signals are small enough, we can decompose the exponential function using the Taylor expansion so (13) can be rewritten as:

$$\begin{aligned} i_{MULT} = \tilde{I}_0 &+ \frac{1}{4}\frac{\tilde{I}_0}{\left(\eta V_T\right)^2}\left[v_{s0}^2 + v_{clk}^2 - 2v_{s0}v_{clk}cos\phi\right] \\ &+ \frac{\tilde{I}_0}{\eta V_T}\left[v_{s0}sin(\omega t - \phi) - v_{clk}sin(\omega t)\right] \\ &- \frac{1}{4}\frac{\tilde{I}_0}{\left(\eta V_T\right)^2}\left[v_{s0}^2 cos(2\omega t - 2\phi) - v_{clk}^2 cos(2\omega t)\right] \\ &- \frac{1}{4}\frac{\tilde{I}_0}{\left(\eta V_T\right)^2}\left[2v_{s0}v_{clk}cos(2\omega t - \phi)\right] \end{aligned} \quad (15)$$

This is the equation equivalent to (4) with two periodic components of frequency f which force the low-pass filter

cut-off frequency to be smaller than that, instead of the $2f$ limit discussed in the previous section. Also, there are DC components which carry no information about ϕ. These components will be removed with a current memory after the low-pass filter.

C. Low-Pass Filter

The output current of the mixer circuit is processed by a low-pass filter to remove frequency components beyond DC. The low-pass filter is highlighted in red in Fig. 2. It is implemented as three current mirrors in series with a capacitance connected to each one of their input nodes (C_1, C_2 and C_3). It also includes at the output a three transistor circuit implementing a cascode stage with an amplifier to increase the output impedance of the circuit [8]. Assuming that all the transistors work in the subthreshold region, their $V_{DS} > 0.1$ V and that all the PMOS and NMOS have the same geometries, the small signal equivalent circuit can be solved, yielding:

$$\frac{i_{out}}{i_{in}} = \frac{g_{mp}\, g_{mp}\, g_{mn}}{(sC_1 + g_{mp})\,(sC_2 + g_{mn})\,(sC_3 + g_{mp})} \tag{16}$$

This is the transfer function of a third order low-pass filter with an unity DC gain. Assuming that the low-pass filter cut-off frequency is smaller than the frequency of the signal, all the periodic components of (15) will be suppressed and the output of this circuit will be:

$$i_{LP} = \tilde{I}_0 + \frac{\tilde{I}_0}{4\,(\eta V_T)^2}\left[v_{s0}^2 + v_{clk}^2 - 2v_{s0}v_{clk}cos\phi\right] \tag{17}$$

It is important to note that even if the periodic terms are not fully suppressed, since they are sinusoidal signals with period T, their integration over a multiple of T is zero so they do not contribute to the final voltage.

D. Current Memory

The current memory is highlighted in green in Fig. 2. The output current from the low-pass filter (17) contains components that do not carry information from the phase of the received light signal, ϕ. These components must be removed before the integration of the current. This is the reason to include the current memory. Before the emission of the light signal, by setting $v_{s0} = 0$ in (17), it can be seen that the output from the low-pass filter is:

$$i_{LP} = \tilde{I}_0 + \frac{1}{4}\frac{\tilde{I}_0}{(\eta V_T)^2}v_{clk}^2 \tag{18}$$

By sampling this current with the current memory this term can be removed and, when the light signal starts to be emitted, only the relevant components will be integrated. The output from the current memory, which is the current being fed to the integrator, will be the subtraction of (18) from (17):

$$i_{LP} = \frac{1}{4}\frac{\tilde{I}_0}{(\eta V_T)^2}\left[v_{s0}^2 - 2v_{s0}v_{clk}cos\phi\right] \tag{19}$$

As explained before, v_{s0} is much smaller than v_{clk}, so the above equation can be approximated by:

$$i_{LOWPASS} = -\frac{1}{2}\frac{\tilde{I}_0 v_{s0} v_{clk}}{(\eta V_T)^2}cos\phi \tag{20}$$

This equation is the equivalent of (5). To reduce the sampling error, this subcircuit is formed by three branches. The one including transistor $M1$ generates a constant current, and the other two are connected to the low-pass output node sequentially, so, the sampling error created in the branch containing transistor $M2$ is absorbed by the branch containing $M3$. All the three branches include a cascode block with an amplifier to increase the output impedance.

E. Integrator

The integrator circuit is highlighted in blue in Fig. 2. It is composed of an inverter, a capacitor and a switch. This circuit is first resetted to a voltage V_{RST}. The geometries of the inverter are designed to fix V_{RST} to a value of around half the voltage supply, i.e. 0.9 V, which leaves room for both positive and negative excursions of the integrated signal. The integration of the current given by (20) is performed during a time interval T_{int}. The final voltage of the circuit will be:

$$v_{OUT1} = V_{RST} - \frac{1}{2}\frac{\tilde{I}_0 v_{s0} v_{clk} T_{int}}{C_{STOR}\,(\eta V_T)^2}cos\phi \tag{21}$$

As explained in the last section, if v_{CLK1} is replaced by v_{CLK2} then (21) changes to:

$$v_{OUT2} = V_{RST} - \frac{1}{2}\frac{\tilde{I}_0 v_{s0} v_{clk} T_{int}}{C_{STOR}\,(\eta V_T)^2}sin\phi \tag{22}$$

And the phase, ϕ, of the signal can be calculated as:

$$\phi_{calc} = atan\left(\frac{V_{RST} - v_{OUT2}}{V_{RST} - v_{OUT1}}\right) \tag{23}$$

IV. Pixel Operation

Each frame of the ToF camera can be divided in two parts: sensing and analog-to-digital conversion. In the first one the integration capacitors are resetted, the current memories sample the signal given by (18) and the integration of the light signal takes place. In the second one the V_{OUT} voltage is digitized. In this paper only the sensing part is taken into account. The time diagram of the relevant control signals for the sensing part of the frame are shown in Fig. 3. We define T_{RST} as the time needed for the integration capacitances to be resetted. As it can be seen, after the reset and before the integration of the light signal, some time is needed for the current memories to perform the sampling operation. This time is labeled in the time diagram as T_{SAMPLE} and the integration time of the light signal as T_{INT}. Their addition is defined as $T_{SUBFRAME}$. To reduce the effect of the sampling error of the memory currents, the sampling process is repeated several times, as it is shown in Fig. 3. As usual, all the reference voltages of the pixel shown in Fig. 2 allow calibration of the sensor to account for PVT variations or systematic errors.

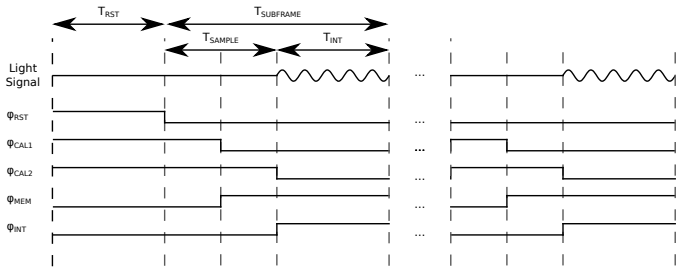

Fig. 3. Time diagram of the sensing period of a single frame.

V. Simulation Resuls

We have run simulations to demonstrate the capacity of the pixel to demodulate the received light signal. Unless stated the contrary all the simulations assume that the light signal being emitted complies with the eye safety regulations [9] and the period of the signal is 50 ns.

Fig. 4 shows a typical nominal result for transient simulations of the pixel during the sensing part of a frame. These results were obtained assuming that the received light signal is reflected from 1 m distance. V_{OFF} shows the value of V_{OUT} without light signal. Ideally, the final value of V_{OUT} would be equal to V_{RST} but, due to non-idealities in the pixel the final value of V_{OUT} differs from V_{RST}. Since these variations do not depend on the received signal or background light, it is enough to sample it once and remove it by replacing V_{RST} with V_{OFF} in (21)-(23). V_{OUT1} and V_{OUT2} show the values of V_{OUT} when (10) and (11) are applied as V_{CLK}.

To test the capacity of the pixel to extract the phase ϕ the simulations shown in Fig. 4 were repeated modifying the phase of the received light signal. These results are summarized in Table V. In this table ϕ_{calc} is calculated applying (23) with the actual values of V_{RST}, i.e. V_{OFF}. As it can be seen, the calculated and real ϕ differ for every value in a constant offset of approximately 26°. This is because the photodiode and the transimpedance amplifier add a phase to the received signal before the demodulation in the mixer. Once again, since this offset does not depend on the light conditions under which the pixel operates a calibration process before the operation would minimize its impact. Once this phase offset

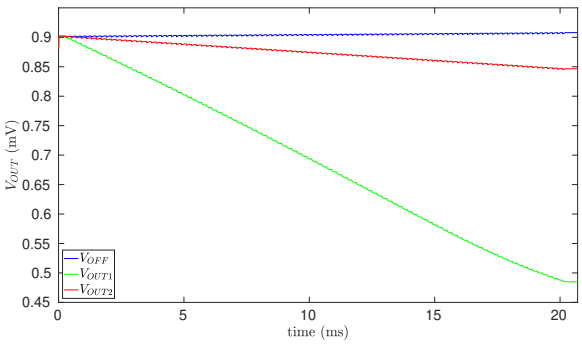

Fig. 4. Transient nominal simulations.

is taken into account (column ϕ_{calc}-26° in Table V) it can be seen that the difference between ϕ and ϕ_{calc} is less than 5°, which is translated in an error of less than 10 cm. It is important to note that the light power of the received signal was assumed constant in these simulations. This decision was made to ensure that any difference between the simulated and calculated ϕ in the simulations is only due to the method of demodulation and the pixel design and not because of the difference in the power level of the received signal.

TABLE I
Comparison between the simulated and calculated ϕ for different ϕ values.

ϕ (°)	V_{OUT1} (mV)	V_{OUT2} (mV)	ϕ_{calc} (°)	ϕ_{calc}-26°	$\Delta\phi$ (°)
18	593	608	46.4	20.3	2.3
36	516	721	64.5	38.3	2.3
54	485	847	81.7	55.6	1.6
72	485	971	98.5	72.4	0.4
90	517	1082	114.0	87.9	-2.1
108	595	1171	130.1	103.9	-4.1
126	712	1232	148.8	122.7	-3.3
144	843	1263	169.6	143.5	-0.5
162	973	1262	190.3	164.2	2.2
180	1088	1230	209.2	183.0	3.0

In addition to these simulations, transient noise simulations were performed. These simulations show a Signal-to-Noise Ratio (SNR) of 20 dB. Most of the noise comes from the sampling error of the current memory. As it has been explained in Section IV the sampling operation of this memory is repeated several times for each frame to reduce the noise figure. In these simulations the integration time was 10 ms and the number of times the sampling operation was performed was 100. Increasing either the integration time or the number of samples will increase the SNR since it is proportianal to the square root of both of them.

VI. Conclusion

This paper has introduced a ToF sensor for standard CMOS technologies with a homodyne demodulation technique for indirect ToF with CW modulation. This technique does not need control signals shorter than the period of the light signal. Thanks to this, switching effects like charge injection and clock feedthrough are minimized and the synchronization issues are avoided. Nominal simulations show that the error in ϕ due to the demodulation technique and pixel design is smaller than 5°, i.e. 10 cm.

Acknowledgment

RTI2018-097088-B-C32 MICINN (FEDER), Xunta de Galicia ED431C2017/69, accreditation 2016-2019, ED431G/08 and FEDER (ERDF), and Xunta de Galicia and the European Union (ESF).

References

[1] T. Spirig, M. Marley, and P. Seitz, "The multitap lock-in CCD with offset subtraction," *IEEE Transactions on Electron Devices*, vol. 44, no. 10, pp. 1643–1647, Oct 1997.

[2] J. Illade-Quinteiro, P. López, V. Brea, D. Cabello, and G. Domnech-Asensi, "Distance Measurement Error in Time-of-Flight Sensors Due to Shot Noise," *Sensors*, vol. 15, pp. 4624–4642, 2015.
[3] M. Beer, B. J. Hosticka, and R. Kokozinski, "SPAD-based 3D sensors for high ambient illumination," in *2016 12th Conference on Ph.D. Research in Microelectronics and Electronics (PRIME)*, June 2016, pp. 1–4.
[4] T. Spirig, P. Seitz, O. Vietze, and F. Heitger, "The lock-in CCD-two-dimensional synchronous detection of light," *IEEE Journal of Quantum Electronics*, vol. 31, no. 9, pp. 1705–1708, Sep 1995.
[5] A. Nemecek, K. Oberhauser, and H. Zimmermann, "Distance measurement sensor with PIN-photodiode and bridge circuit," *IEEE Sensors Journal*, vol. 6, no. 2, pp. 391–397, April 2006.
[6] S. J. Kim, J. D. K. Kim, B. Kang, and K. Lee, "A CMOS Image Sensor Based on Unified Pixel Architecture With Time-Division Multiplexing Scheme for Color and Depth Image Acquisition," *IEEE Journal of Solid-State Circuits*, vol. 47, no. 11, pp. 2834–2845, Nov 2012.
[7] C. Bamji and E. Charbon, "Systems for cmos-compatible three-dimensional image sensing using quantum efficiency modulation," Patent US 6 580 496B2, 06 17, 2003. [Online]. Available: https://patents.google.com/patent/US6580496B2/
[8] B. Razavi, *Design of Analog CMOS Integrated Circuits*, 2nd ed. CGraw-Hill, 2001.
[9] "Safety of laser products - Part 1: Equipment classification and requirements," IEC 60825-1:2014, 2014.